

POST PRINT

<https://www.sciencedirect.com/science/article/abs/pii/S0308814618305612>

<https://doi.org/10.1016/j.foodchem.2018.03.120>

Food Chemistry, Volume 259, 2018, Pages 139-146, ISSN 0308-8146,

Utilization of a freeze-thaw treatment to enhance phenolic ripening and tannin oxidation of grape seeds in red (*Vitis vinifera* L.) cultivars

Laura Rustioni¹, Gabriele Cola¹, Josh VanderWeide², Patrick Murad², Osvaldo Failla¹ and Paolo Sabbatini²

¹ DISAA e Dipartimento di Scienze Agrarie e Ambientali, Università Degli Studi di Milano, Via Celoria 2, 20133 Milano, Italy

² Department of Horticulture, Plant & Soil Sciences Building, Michigan State University, East Lansing, MI, 48824

Abstract

Phenolic ripening represents a major interest for quality wine producers. Nevertheless, climatic or genotypical limitations can often prevent optimal maturation process. During winemaking seeds can be easily separated and technologically processed to improve their quality. Relying on the key role of oxidation for phenolic ripening, a freeze-thaw treatment was proposed to improve the fruit quality for potential use in challenging growing conditions. The experiment was carried on in two distinctive viticultural areas, Michigan and Italy. Five cultivars (Cabernet Franc, Cabernet Sauvignon, Merlot, Pinot noir and Chambourcin) and six cultivars (Cabernet Sauvignon, Sangiovese, Syrah, Croatina, Barbera and Nebbiolo) were used in Michigan and Italy, respectively. Samples were collected at different phenological stages, to describe the natural ripening process and grape seeds were characterized before and after a freeze-thaw treatment. Colorimetric and spectrophotometric data highlighted similarities among natural and artificial seed ripening promising future applications for the wine industries.

Keywords: viticulture; oenology; artificial ripening; suboptimal climate; winemaking

Funding: *This research did not receive any specific grant from funding agencies, public or private, or not-for-profit sectors.*

35 1. INTRODUCTION

36 The importance of seed color at harvest time for grape quality evaluation has been understood for
37 millennia – the famous Roman agriculture writer Columella (4-70 A.D.) suggested the process of seed
38 darkening as the best grape ripening index in his book: “De Re Rustica” (Rustioni & Failla, 2016).
39 During ripening, a grape seed starts as a bright green color, and slowly changes to yellow, and
40 eventually dark brown shades (Ristic & Illand, 2005; Ferrer-Gallego, García-Marino, Hernández-
41 Hierro, Rivas-Gonzalo & Escribano-Bailón, 2010; Rodríguez-Pulido, Gómez-Robledo, Melgosa,
42 Gordillo, González-Miret & Heredia, 2012). The seed coat modifications during ripening aims to
43 provide mechanical protection to the embryo and to maintain seed dormancy (Ristic & Illand, 2005;
44 Rolle, Giacosa, Torchio, Perenzoni, Rio Segade, Gerbi & Mattivi 2013). Seed browning during berry
45 ripening is considered to be the result of oxidation of flavan-3-ols and tannins (Kennedy, Matthews &
46 Waterhouse, 2000; Adams, 2006; Ristic & Illand, 2005; Rustioni & Failla, 2016), which are initiated
47 by an oxidative burst at veraison (Pilati et al., 2007). The major role of phenolic oxidation in coat
48 browning has been shown to occur during the development of seeds and fruits in different species
49 including *Arabidopsis thaliana*; *Phaseolus vulgaris*; *Zea mays*; *Litchi chinensis* (Pourcel et al., 2007).

50 In addition to tannin color, the oxidation of phenolics is expected to affect their gustatory
51 perception, including astringency (McRae & Kennedy, 2011). It is well known that astringency
52 perception is a complex tactile sensation caused by a loss of lubricity in oral saliva (McRae & Kennedy,
53 2011; Cheynier et al., 2006). The interactions between tannins and saliva proteins that are responsible
54 for this perception involve a number of mechanisms, including hydrophobic interactions (Van der
55 Waals and π - π stacking), hydrogen bonding, self-association (causing cross-links between protein-
56 tannin complexes) and finally, protein aggregation and eventual production of colloidal particles
57 (McRae & Kennedy, 2011). Through the formation of new bonds, and the modification of the molecular
58 structures and interactions (McRae & Kennedy, 2011; Pourcel et al., 2007), intra-molecular bonding is
59 increased, which reduces tannin flexibility; altering linear and extended tannin forms into more
60 condensed structures (Poncet-Legrand et al., 2010; McRae & Kennedy, 2011). Flavanol polymerization
61 reactions, regardless of the polymers formed (proanthocyanidins, oxidation products, or ethylflavanols),
62 generally enhance the astringency (Cheynier et al., 2006). Nevertheless, the availability of binding sites
63 (associated to the structural flexibility) and the steric hindrance of the tannin polymer could prevent the
64 protein access to binding sites, creating a threshold in the correlation among tannin size and protein
65 binding efficacy (McRae & Kennedy, 2011).

66 Despite the current knowledge of seed color and tannin oxidation, and their relationship to fruit
67 quality and wine making, environmental conditions pose a challenge to their development in different
68 viticultural areas: ideal growing conditions for *Vitis vinifera* consist of temperate climate regions with
69 warm, dry summers seeing moderate precipitation, and mild winters. The first challenge is the increase
70 in heat accumulation in warm viticultural grape growing regions, which is prominent in many Italian
71 vineyards. Increased summer temperatures are capable of altering the pathways of secondary

72 metabolites during ripening, resulting in poor polyphenolic maturation and low fruit quality at harvest
73 (Frioni, Zhuang, Palliotti, Sivilotti, Falchi & Sabbatini, 2017)The second challenge is the annual
74 variation in climatic conditions experienced in many cool climate viticultural regions, including
75 Michigan. Each issue can be associated with global climate change, and they are limiting the sustainable
76 production of grapes with a consistent optimal fruit quality at harvest in several viticultural areas of the
77 world (Schultze, Sabbatini & Luo, 2016).

78 Technological procedures targeted towards improving phenolic oxidations are widespread
79 among wine producers located in suboptimal environmental climates. The most prominent examples
80 include: must oxygenation during maceration, use of wood barrels and, in general, wine micro-
81 oxygenation (Gómez-Plaza & Cano-López, 2011). The main restriction of these techniques concerns
82 the non-selective nature of tannin oxidation obtained through musts and wines, which involves
83 interactions with other molecules that potentially affect additional organoleptic characteristics (e.g.
84 accumulation of aldehydes). The oxidation effects on different wines has been described by Bueno,
85 Culleré, Cacho, & Ferreira (2010).

86 Phenols are predominantly located in the vacuole, while oxidoreductases are found in the
87 cytoplasm. Thus, their interaction, and subsequent induction of enzymatic browning will not occur
88 unless the cell membranes are damaged (Li, Guo & Wang, 2008). Freeze-thaw treatments are known to
89 affect the ultrastructure of vacuolated cells, due to the formation of ice crystals during freezing, which
90 affect membranous components of the protoplasm (Mohr & Stein, 1969). This process has previously
91 been observed in studies focused on strawberry shelf-life managements (Oszmiański, Wojdyło &
92 Kolniak, 2009; Holzwarth, Korhummel, Carle & Kammerer, 2012). Considering grape seeds, different
93 techniques are already available to separate them from the must during winemaking (Canales, Llaudy,
94 Canals & Zamora, 2008). Nevertheless, the seed removal (recommended in case of suboptimal phenolic
95 ripening) could also impoverish wines in terms of ‘body’ and ‘structure’, eliminating a tannin source.
96 Thus, in our opinion, seed recycling after freeze-thaw treatment, could be recommended to improve
97 wine quality.

98 Phenolic heterogeneous pigments obtained by free radical polymerization caused by oxidations
99 (Waterhouse & Laurie, 2006) are difficult to be quantified by traditional chemical assays due to their
100 inhomogeneity and extractability limitations. For example, the oxidation bonds are resistant to acid
101 catalyzed thiolysis (Kennedy et al., 2000) and the tannin oxidation can lead to solubility problems
102 (Poncet-Legrand et al., 2010; Zanchi et al., 2007). Nevertheless, the presence of conjugated double
103 bonds in these phenolic oxidized molecules allows the absorption of light of visible wavelengths
104 (Rustioni, 2017). In fact, the spectrum of oxidized polymeric phenolics was recently characterized in
105 sunburn grape berries, indicating a broad absorption band in the green spectral region, with a maximum
106 around 500 nm (Rustioni, Rocchi, Guffanti, Cola & Failla 2014). Therefore, the optical properties of
107 seeds measured on-solid could be impacted by the detection limitations of the oxidized polymeric
108 phenolics. However, CIELab color parameters and image analysis have already been proposed as a

109 technique to evaluate seed ripening (Obreque-Slier, López-Solís, Castro-Ulloa, Romero-Díaz & Peña-
110 Neira, 2012; Ferrer-Gallego et al., 2010; Rodríguez-Pulido et al., 2012).

111 The present study aims to test a new procedure based on the selective oxidation of grape seeds
112 by a physical treatment (freezing) to improve tannin ripening. Modifications to the seed's optical
113 properties that occur during natural ripening and freezing treatment will be investigated and described
114 using two different analytical approaches (spectrophotometric and colorimetric), and will utilize grape
115 cultivars grown in two viticultural areas (Italy and Michigan).

116

117 2. MATERIALS AND METHODS

118

119 2.1. Environmental characteristics

120 The experiment was carried out during the 2017 growing season in the United States (Michigan)
121 and Italy. Benton Harbor, Michigan (Latitude 42.0841 deg, Longitude - 86.3570 deg, Elevation: 220
122 m) and Riccagioia, Italy (Latitude 44.98; Longitude 9.08; Elevation 144) are characterized by different
123 climates. Following the Köppen-Geiger Classification (Köppen, 1936), Benton Harbor's climate is
124 under the Dfa type: continental without dry season with hot summer, while Riccagioia is Cfb: temperate
125 without dry season with warm summer. The following agro-climatological analysis were completed
126 using data collected from weather stations located near the experimental vineyards. The Benton Harbor
127 weather station is a part of Enviro-weather, a weather station network run by Michigan State University,
128 and is located 14 km far from the commercial vineyard in the Lake Michigan Shore AVA (American
129 Viticulture Area) where samples were collected. Torrazza Coste station, 1 km far from the Riccagioia
130 experimental field, belongs to the network of Consorzio Tutela Vini Oltrepò Pavese, the local wine-
131 growers consortium. Data were analyzed for the period 2000, January 1st – 2017, October 31st. In order
132 to provide an evaluation of the availability of thermal resources during the different phases of the
133 growing season two methods of analysis were used:

134 1 - GDD - Winkler Growing Degree Days (Amerine & Winkler, 1944)

135 2 – NHH – Normal Heat Hours (Cola et al., 2014, Parisi et al., 2014)

136 The advantage of NHH over GDD is the use of a response curve considering optimal temperature for
137 grape growth, taking into account the negative effects of under and over-optimal temperatures on plant
138 growth (Mariani et al., 2012).

139 Figure 1 displays these patterns from 2000-2017; blue and red lines represent the average value for
140 Benton Harbor (Michigan) and Riccagioia (Italy), respectively, in terms of the seven Winkler classes.
141 The average value for Benton Harbor was 1576 GDD, which follows the Winkler class II: temperate
142 cool, suitable for early ripening grapes for wines to be aged, and medium ripening grapes for white or
143 red wines ready to drink. Riccagioia, with an average value of 2119 GDD, falls into class IV: temperate
144 warm, suitable for late ripening grapes for white or red wines ready to be aged. The difference in thermal
145 resources availability of the two areas is confirmed by the analysis of figure 2, where ten-day

146 accumulations of GDD (a1 and a2) and NHH (b1 and b2) are presented. Red lines represent 2017
147 behavior, and thick, black lines indicate average 2000-2016 values. The dark grey area is bordered by
148 an average ± 1 standard deviation and the light gray area by an average ± 2 standard deviation. The
149 timespan between fruit-set and physiological maturity is represented by the purple area.

150

151 **2.2. Plant material and experimental design**

152 In Michigan, 5 cultivars were considered: Cabernet Franc, Cabernet Sauvignon, Merlot, Pinot
153 noir (*Vitis vinifera* L.) and the French-American hybrid Chambourcin (Seyval-Villard 12-417 \times
154 Chancellor). Samples (3-5 bunches) of each cultivar were collected at the beginning of ripening (T0 -
155 BBCH 85) and harvest time (T2 - BBCH 88) from a commercial grower collection (Meier, 2001). In
156 Italy, vines were used from the ampelographic collection located in Oltrepò Pavese (south Lombardy),
157 described in Rustioni, Basilico, Fiori, Leoni, Maghradze and Failla (2013). Six (*Vitis vinifera* L.)
158 cultivars (Cabernet Sauvignon, Sangiovese; Syrah; Croatina; Barbera and Nebbiolo) were considered.
159 Samples (3-5 bunches) of each cultivar were collected at veraison (T0 - BBCH 83); middle ripening
160 (T1 - BBCH 86); and harvest time (T2 - BBCH 89) (Meier, 2001).

161 At both research institutes, clusters were analyzed within 24 hours of the sampling time. 50 seeds
162 were randomly selected from each cultivar, and linearly arranged on a polystyrene board to maintain
163 the seeds in position. Each seed was analyzed immediately after placement on the board, and after the
164 freezing treatment. The procedure consisted of freezing (-20°C) the seeds overnight, followed by a 3-
165 hour defrosting period at room temperature. A total of 1,400 seeds were analyzed at two points during
166 the experiment.

167

168 **2.3. Data records, data elaboration and statistical analysis**

169 Analyses were carried out using a Konica Minolta Chroma Meter CR-400 (Konica Minolta, Osaka,
170 Japan) in Michigan, and a Jaz System spectrometer (Ocean Optics, B.V., Dunedin, USA) in Italy. Seeds
171 were described by 3 colors parameters: lightness (L*), chroma (C*) and hue (h*). The L* parameter
172 ranges from 100 (perfect white) and zero (black) (Obreque-Slier et al., 2012). The C* parameter
173 increases with chromatic saturation. The h* parameter, indicates the tone or hue and is expressed in
174 angle degrees (0° = red; 90° = yellow; 180° = green; 270° = blue)
175 (<http://sensing.konicaminolta.us/2015/03/understanding-the-cie-lch-color-space/>). The changes to
176 these parameters in each seed before and after treatment are representative of the artificial ripening
177 effect. Variation in the color of each ripened seed (T2) with respect to the cultivar's average seed color
178 at T0 are indicative of natural ripening effects. The Jaz System spectrometer (Ocean Optics, B.V.,
179 Dunedin, USA) was fitted with a DPU module, an ILX511b detector, an OFLV-3 filter, an L2 lens, and
180 a 50 μ m slit as installed options. A reflection probe QR600-7-VIS125 consisting of a tight bundle of
181 seven optical fibers (600 μ m in diameter) in a stainless-steel ferrule (six illumination fibers around one
182 read fiber), was coupled to the spectrophotometer. A probe holder was included to ensure the analytical

183 reproducibility - the distance between the sample surface and the probe was fixed at 12 mm. The
184 instrument was set up with a near infrared– visible (NIR–vis) light source (Ocean Optics) 4095 power
185 setting, and an integration time automatically corrected by the instrument. Collected spectra ranged
186 between 341 and 1025 nm and had a spectral resolution of approximately 0.3 nm. Each spectrum was
187 set up to be the average of 15 spectra, which were directly calculated by the instrument. A calibration
188 with a blank was obtained using a polytetrafluoroethylene (PTFE) diffuse reflectance standard (Ocean
189 Optics B.V.). Reflectance spectra were first elaborated using the script reported in Rustioni, Ciacciulli,
190 Grossi, Brancadoro and Failla (2016) by R software (R Core Team). This initial data processing allowed
191 the spectra (400-800 nm) to be transformed to a percentage with respect to the blank; and the
192 normalization at 800 nm (N800). Next, the N800 reciprocal was calculated, obtaining the $1/N_{800}$ spectra
193 to approximate the graphs at the absorption spectra. Then, to highlight pigment variation as a
194 consequence of the treatment, the initial spectrum was subtracted from the post-treatment spectrum for
195 each seed. The compositional modifications during ripening were described by subtracting the average
196 T0 seed spectrum of each cultivar to the spectra recorded at T1 and T2 sampling times. Statistical
197 variability of the spectra was evaluated by considering the error bars (95% CI). Statistical analyses were
198 obtained by using Microsoft Office Excel and SPSS statistical software (version PASW Statistics 24,
199 SPSS, Inc. Chicago, IL).

200

201 3. RESULTS AND DISCUSSION

202

203 3.1. Natural maturity of seeds in Michigan

204 Regarding the colorimetric analysis of seeds collected in Michigan, the analysis of variance
205 highlighted significant effects (Significance = 0.000) of the cultivar, sampling time and cultivar *
206 sampling time interaction for all the variables considered (L^* ; C^* and h^*). Only the L^* value showed a
207 lower significance (0.004) concerning the cultivar * sampling time interaction. Table 1a reports the seed
208 color variations in terms of average values and individual cultivars. The variation in lightness (L^*)
209 values could be attributed to physical modifications of the seed surface, probably related to mechanical
210 protection and seed dormancy maintenance. Considering the chroma and hue, we observed an increase
211 in the C^* and h^* values in all cultivars (with the exception of h^* in Cabernet Sauvignon). This trend
212 indicates a shift towards intense yellow colors ($h^* \approx 90$ and higher color saturation defined by higher
213 C^* values), and could be ascribed to the oxidized phenolics responsible for the main absorption band
214 (490 nm – 510 nm) shown in Figure 3a and described in the following paragraph (3.3). Nevertheless,
215 natural ripening of grapes of these cultivars in Michigan did not appear to produce highly polymerized
216 reddish-brown pigments in seeds. The lower seasonal temperature accumulation (GDD and NHH)
217 (paragraph 2.1) observed in this growing region compared with Italy is likely to be the cause.

218 Michigan, a cool climate viticulture region, is characterized by short and variable summers, and
219 rain is often heavy during the final months of maturation. In Michigan, environmental conditions that

220 influence ripening are highly variable from year to year. According to the Winkler GDD scale,
221 Michigan's two primary growing regions, Northwest and Southwest, fall into regions 1a-1b and regions
222 1a-III. This variability indicates that the capability of grapes to reach full maturity on a consistent basis
223 is restricted in most seasons due to lack of adequate temperature accumulation. For this reason, fruit
224 technological maturity at harvest can be reduced by slow maturation dynamics. A favorable shift in
225 climatic conditions has occurred over the past decades that has led to an increase in vinifera cultivated
226 area, especially in cultivars internationally renowned (e.g. Italy, France, USA) for high quality wine
227 production such as Merlot, Pinot noir and Cabernet Sauvignon. Despite continuous extension of grape
228 vegetative season length due to climate change, seasonal variability is expected to be more stable in the
229 future. This suggests the need for a solution that moderates the impact of low seasonal temperature
230 accumulation, especially for red *Vitis vinifera* cultivars, that heavily rely on consistent heat units to
231 reach full technological maturity t harvest. Even if several viticultural techniques can be adopted to
232 mitigate the effects of climatic constraints on fruit quality, they have a limited impact on increasing
233 polyphenols concentration of the fruit at harvest (Frioni et al, 2017).

234

235 **3.2. Natural maturity of seeds in Italy**

236 Variations of seed reflectance spectra in time, were used in the Italian samples to characterize the
237 phenolic oxidations that occurred during fruit ripening (Figure 3). In Figure 3a, a spectrum representing
238 the average values of all the considered cultivars at each sampling time can be observed. The band
239 peaking at 678 nm is ascribed to chlorophylls (Merzlylyak, Solovchenko & Gitelson, 2003; Rocchi,
240 Rustioni & Failla, 2016), which significantly decreased between the first and second sampling, and
241 remained constant until harvest. Figure 3b indicates that chlorophyll degradation in seeds is not
242 ubiquitous among all the studied cultivars. In Barbera and Sangiovese, no significant differences at 678
243 nm were recorded. This is most likely due to the low initial concentrations (Figures SI1 a.4 and a.5).
244 During ripening, the seed color changes, starting with a bright green, through green-yellow to yellow
245 and then through yellow-brown to dark brown colors (Ristic and Illand, 2005). These same
246 pigmentation changes were observed in all our samples. Thus, the degradation of chlorophyll pigments
247 does not appear to play a crucial role in seed coat ripening; despite the quantity of chlorophyll, a brown
248 color was obtained.

249 In Figure 3a, the main absorption band (490 nm – 510 nm) is responsible for the yellowish-brownish
250 color of the seed coat (absorbance in the green spectral region). This band is similar to the ones in
251 grapevine woody tissues (Grossi, Rustioni, Simone Di Lorenzo, Failla & Brancadoro, 2016) and
252 sunburned grape berry skins (Rustioni et al., 2014) and it is characteristic of oxidized polymeric
253 phenolics, consistent with the expected physiological oxidations of grape seed coat (Kennedy et al.,
254 2000; Adams, 2006; Ristic and Illand, 2005; Rustioni and Failla, 2016; Pourcel et al., 2007).

255 This main band underwent both hyperchromic and bathochromic shifts during ripening (Figure 3a).
256 Furthermore, an increased asymmetry of the main band was observed due to an increased absorbance

257 in the right shoulder (≈ 570 nm). The hyperchromic shift can easily be explained by the increased
258 concentration of brown pigments due to phenolic oxidations during ripening (Pourcel et al., 2007;
259 Kennedy et al., 2000; Adams, 2006; Ristic and Illand, 2005; Rustioni and Failla, 2016). The
260 bathochromic shift is accentuated in the Figure 3b representation, in which the differential spectra
261 between T2 and T0 samples in each cultivar is shown. The data indicates the prevalence of accumulation
262 of reddish-brown pigments in all the cultivars during ripening. A broad absorption band in the green
263 region (≈ 430 -660 nm) and a maximum absorption around 570 nm characterizes these colored
264 compounds. Depending on the cultivar considered, this band could appear thinned, however this should
265 be ascribed to the negative contribution of chlorophyll degradation, indicated by the spectral negative
266 bands in the red (peak at 678 and shoulder at 650 nm) and in the blue (around 430 nm) regions. In
267 general, the bathochromic shift observed during ripening (490-510 nm) and the observed intensification
268 of the shoulders at higher wavelengths (≈ 570 nm) indicate a decrease in the radiative energy required
269 for the electron excitation of brown pigments. Generally, bathochromic shifts of the absorption bands
270 results from increases in the molecular complexity (e.g.: number of conjugated bonds and substituents)
271 (Cockell & Knowland, 1999; Rustioni, Di Meo, Guillaume, Failla & Trouillas, 2013). Continuous
272 oxidations take place during the ripening season, and they are consistent with an increase of the number
273 of conjugated rings in brown pigments. In fact, after oxidations, quinones undergo phenolic
274 regenerations and could be easily involved in further polymerizations, as they phenolic oxidation
275 products are more readily oxidized than their precursors (Li et al., 2008; Pourcel et al., 2007;
276 Waterhouse & Laurie, 2006; Adams, 2006).

277

278 **3.3. Freeze-thaw treatment and artificial seed ripening – colorimetric characterization**

279 With the aim of improving seed phenolic ripening in suboptimal climatic conditions, the effect of
280 a freeze-thaw treatment on seed color was evaluated in Michigan. The analysis of variance highlighted
281 significant effects (Significance = 0.000) of the treatment, cultivar, sampling time and their interactions
282 for all the variables considered (L^* ; C^* and h^*). The L^* value showed a slightly lower significance in
283 the sampling time x treatment and sampling time x treatment x cultivar interactions (significance 0.003
284 and 0.001 respectively). The C^* value showed a slightly lower significance in the sampling time x
285 treatment; treatment x cultivar and sampling time x treatment x cultivar interactions (significance 0.011;
286 0.009 and 0.001 respectively).

287 The treatment effect on the seed color is summarized in table 1b. The artificial ripening process
288 produced a decrease in lightness (L^*), but not significantly in all the cultivars and sampling times
289 considered. The physical damages of the seed coat caused by the defrosting procedures (Mohr & Stein,
290 1969) could be responsible of the lightness variations. Considering the chroma and hue (C^* and h^*),
291 we consistently observed a significant decrease in those values due to the treatment, with the exception
292 of the first sampling time of Chambourcin grapes. The values clearly indicate a browning effect of the
293 freeze-thaw treatment, and, thus, the production of reddish-brown pigments. The visual inspection of

294 the seeds was also coherent with the traditionally recognized darkening characteristic of the ripening
295 process (Rustioni & Failla, 2016; Ristic & Illand, 2005; Ferrer-Gallego et al., 2010; Rodríguez-Pulido
296 et al., 2012). Nevertheless, seed color variations obtained with the artificial treatment appeared to be
297 slightly different in relation to the color modifications observed during the natural fruit ripening .
298

299 **3.4. Freeze-thaw treatment and artificial seed ripening – spectrophotometric characterization**

300 To understand the freeze-thaw treatment effects on oxidized phenolics, allowing a comparison with
301 the naturally ripen pigmentation, the seed reflectance spectra were studied on the Italian samples. Figure
302 4 details the modifications in seed pigmentation obtained by reflectance spectroscopy in the Italian
303 samples. Figure 4a shows the average seed spectra before and after treatment in the three sampling
304 times. It is interesting to note that the freeze-thaw procedure generally intensified the absorption bands
305 (hyperchromic shifts), without affecting the spectral profile of each phenological phase. This means
306 that the treatment enhanced the production of the pigments characteristic of each phenological phase,
307 but did not strongly affect their molecular conformation. Observing the differential spectra ($\Delta(1/N_{800})$ -
308 Figure 4b), it is possible to compare the variations due to ripening (red lines) and treatment (blue lines).
309 As previously described in the 3.2 paragraph, ripening produced a broad absorption band, spread in the
310 entire visible spectrum, with a maximum around 540 nm. The bands obtained by the freeze-thaw
311 treatments did not perfectly overlap with the ones produced by natural ripening. Furthermore, the
312 bathochromic shift of the absorption band ascribable to the treatment can be observed, moving from
313 T0, through T1 to T2 (having peak maximum around 475 nm; 500 nm and 605 nm respectively). These
314 data suggest a major role of phenology-specific enzymatic oxidations. In fact, the cell
315 decompartmentalization caused by the treatment (Mohr and Stein, 1969) would induce phenolic
316 oxidations; nevertheless, the compounds obtained are similar to the ones naturally formed in each
317 phenological stage supporting the hypothesis of enzymatic reactions. In spite of this, the treatment set
318 up in terms of temperatures and timing for each cultivar could address the biochemical oxidation toward
319 the target results. For example, considering Nebbiolo grapes (Figure 5), the treatment at veraison
320 induced the formation of the same compounds obtained during ripening, independent of the original
321 phenological phase. Further details concerning the cultivar-specific response to the treatment are
322 available in supplementary information (SI1).

323

324 **4. CONCLUSIONS**

325 Phenolic ripening represents a major interest for quality wine producers. Nevertheless, climatic or
326 genotypical restrictions can prevent the optimal maturation process. Relying on the key role of oxidation
327 for phenolic ripening, a freeze-thaw treatment was proposed to improve the grape quality for potential
328 use in suboptimal growing conditions. The data summarized here highlight pigment formation between
329 natural and artificial ripening systems, however, some differences were evident, most likely due to the
330 degree of oxidative polymerizations. Further studies should focus on the optimization of seed collection,

331 freezing temperatures, and impact on wine sensory analysis, taking into consideration the cultivar-
332 specific responses.

333 From an application perspective, this technique could be tested at the industrial scale. Currently, a
334 number of techniques are available to separate grape seeds from the must (Canales et al., 2008).
335 Furthermore, the freeze-thaw treatment does not rely on the use of chemical additives, which can be a
336 concern for winemakers. For the freezing process, the use of dry ice - easily available in mostly of the
337 winegrowing regions - could represent the best compromise in terms of costs and industrial
338 management. In a medium sized cellar, seeds could be simply separated by precipitation in a tank or
339 vat, during pump-overs. A freezing treatment of the seeds could be applied directly to the fermentation
340 tanks adding dry ice, allowing the thawing process at room temperature. Nevertheless, additional
341 research could discover a technological solution more suitable for industrial winemaking. Temperature
342 control and timing of the freeze-thaw treatments, could be also of primary importance to address the
343 artificial ripening process to the best cultivar specific treatment conditions.

344

345 REFERENCES

- 346 1. Adams, D.O. (2006). Phenolics and ripening in grape berries. *Am. J. Enol. Vitic.*, 57(3), 249-
347 256.
- 348 2. Amerine, M.A., & Winkler, A.J. (1944). Composition and quality of must and wines of
349 California grapes. *Hilgardia*, 15, 493-675.
- 350 3. Bueno, M., Culleré, L., Cacho, J., & Ferreira, V. (2010). Chemical and sensory characterization
351 of oxidative behavior in different wines. *Food Research International*, 43(5), 1423-1428.
- 352 4. Canales, R., Llaudy M.C., Canals J.M., & Zamora F. (2008). Influence of the elimination and
353 addition of seeds on the colour, phenolic composition and astringency of red wine. *Eur Food*
354 *Res Technol*, 226, 1183–1190.
- 355 5. Cheynier, V., Dueñas-Paton, M., Salas, E., Maury, C., Souquet, J.M., Sarni-Manchado, P., &
356 Fulcrand H. (2006). Structure and Properties of Wine Pigments and Tannins. *Am. J. Enol. Vitic.*,
357 57(3), 298-305.
- 358 6. Cockell, C.S., & Knowland, J. (1999). Ultraviolet radiation screening compounds. *Biol. Rev.*
359 *Cambridge Philos. Soc.*, 74, 311–345.
- 360 7. Cola, G., Mariani, L., Salinari, F., Civardi, S., Bernizzoni, F., Gatti, M., & Poni S. (2014).
361 Description and testing of a weather-based model for predicting phenology, canopy
362 development and source-sink balance in *Vitis vinifera* L. cv. Barbera. *Agricultural and forestry*
363 *Meteorology.*, ISSN: 0168-1923, doi: 10.1016/j.agrformet.2013.09.008, 117-136.
- 364 8. Columella, L.G.M. (4-70 A.D.) De re rustica, liber undecimus.
- 365 9. Ferrer-Gallego, R., García-Marino, M., Hernández-Hierro, J.M., Rivas-Gonzalo, J.C., &
366 Escribano-Bailón, M.T. (2010) Statistical correlation between flavanolic composition, colour
367 and sensorial parameters in grape seed during ripening. *Analytica Chimica Acta*, 660, 22–28.

- 368 10. Frioni, T., Zhuang, S., Palliotti, A., Sivilotti, P., Falchi, R., & Sabbatini, P. (2017). Leaf
369 Removal and Cluster Thinning Efficiencies Are Highly Modulated by Environmental
370 Conditions in Cool Climate Viticulture. *American Journal of Enology and Viticulture*, 68, 325-
371 335.
- 372 11. Gómez-Plaza, E., & Cano-López M. (2011). A review on micro-oxygenation of red wines:
373 Claims, benefits and the underlying chemistry. *Food Chemistry*, 125(4), 1131-1140.
- 374 12. Grossi, D., Rustioni, L., Simone Di Lorenzo, G., Failla O., & Brancadoro L. (2016). Water
375 deficit effects on grapevine woody tissue pigmentations. *Hort. Sci. (Prague)*, 43(4), 188–194.
- 376 13. Holzwarth, M., Korhummel, S., Carle, R., & Kammerer D.R. (2012). Evaluation of the effects
377 of different freezing and thawing methods on color, polyphenol and ascorbic acid retention in
378 strawberries (*Fragaria × ananassa* Duch.). *Food Research International*, 48, 241–248.
- 379 14. Kennedy, J.A., Matthews, M.A., & Waterhouse, A.L. (2000). Changes in grape seed
380 polyphenols during fruit ripening. *Phytochemistry*, 55(1), 77-85.
- 381 15. Köppen, W. (1936). *Das geographische System der Klimate. Handbuch der Klimatologie*. 1. In
382 Köppen, Wladimir; Geiger (publisher), Rudolf. Berlin: Borntraeger.
- 383 16. Li, H., Guo, A., & Wang, H. (2008). Mechanisms of oxidative browning of wine. *Food Chem.*,
384 108, 1–13.
- 385 17. Mariani, L., Parisi, S.G., Cola, G., & Failla, O. (2012). Climate change in Europe and effects
386 on thermal resources for crops. *International Journal of Biometeorology*, 56(6), 1123-1134.
- 387 18. McRae, J.M., & Kennedy, J.A. (2011). Wine and Grape Tannin Interactions with Salivary
388 Proteins and Their Impact on Astringency: A Review of Current Research. *Molecules*, 16,
389 2348-2364.
- 390 19. Meier, U. (2001). *Growth Stages of Mono- and Dicotyledonous Plants BBCH. Monograph*, 2nd
391 ed. Federal Biological Research Centre of Agriculture, Germany.
- 392 20. Merzlylyak, M. N., Solovchenko, A. E., & Gitelson, A. A. (2003). Reflectance spectral features
393 and non- destructive estimation of chlorophyll, carotenoid and anthocyanin content in apple
394 fruit. *Postharvest Biol. Technol.*, 27, 197-211.
- 395 21. Mohr, W.P., & Stein, M. (1969). Effect of different freeze-thaw regimes on ice formation and
396 ultrastructural changes in tomato fruit parenchyma tissue. *Cryobiology*, 6(1), 15-31.
- 397 22. Obreque-Slier, E., López-Solís, R., Castro-Ulloa, L., Romero-Díaz, C., & Peña-Neira, A.
398 (2012). Phenolic composition and physicochemical parameters of Carménère, Cabernet
399 Sauvignon, Merlot and Cabernet Franc grape seeds (*Vitis vinifera* L.) during ripening. *LWT -*
400 *Food Science and Technology*, 48, 134-141.
- 401 23. Oszmiański, J., Wojdyło, A., & Kolniak, J. (2009). Effect of L-ascorbic acid, sugar, pectin and
402 freeze–thaw treatment on polyphenol content of frozen strawberries. *LWT - Food Science and*
403 *Technology*, 42, 581–586.

- 404 24. Parisi, S.G., Antoniazzi, M.M., Cola, G., Lovat, L., Mariani, L., Morreale, G., Zoltan, K., &
405 Calò, A. (2014). Spring thermal resources for grapevine in Koszeg (Hungary) deduced from a
406 very long pictorial time series (1740-2009). *Climatic Change*, *126*, 443-454.
- 407 25. Pilati, S., Perazzolli, M., Malossini, A., Cestaro, A., Demattè, L., Fontana, P., Dal Ri, A., Viola,
408 R., Velasco, R., & Moser C. (2007). Genome-wide transcriptional analysis of grapevine berry
409 ripening reveals a set of genes similarly modulated during three seasons and the occurrence of
410 an oxidative burst at veraison. *BMC Genomics*, *8*, 428.
- 411 26. Poncet-Legrand, C., Cabane, B., Bautista-Ortín, A., Carrillo, S., Fulcrand, H., Pérez, J., &
412 Vernhet, A. (2015). Tannin oxidation: Intra- versus intermolecular reactions.
413 *Biomacromolecules*, *11*, 2376-2386.
- 414 27. R Core Team. (2015). *R: A Language and Environment for Statistical Computing*; R
415 Foundation for Statistical Computing: Vienna, Austria; <https://www.R-project.org/>.
- 416 28. Ristic, R., & Iland, P.G. (2005). Relationships between seed and berry development of *Vitis*
417 *vinifera* L. cv Shiraz: developmental changes in seed morphology and phenolic composition.
418 *Australian Journal of grape and wine research*, *11*, 43-58.
- 419 29. Rocchi, L., Rustioni, L., & Failla O. (2016). Chlorophyll and carotenoid quantifications in
420 white grape (*Vitis vinifera* L.) skins by reflectance spectroscopy. *Vitis*, *55*, 11–16.
- 421 30. Rodríguez-Pulido, F., Gómez-Robledo, L., Melgosa, M., Gordillo, B., González-Miret, M.L.,
422 & Heredia, F.J. (2012). Ripeness estimation of grape berries and seeds by image analysis.
423 *Computers and Electronics in Agriculture*, *82*, 128–133.
- 424 31. Rolle, L., Giacosa, S., Torchio, F., Perenzoni, D., Río Segade, S., Gerbi, V., & Mattivi F.
425 (2013). Use of Instrumental Acoustic Parameters of Winegrape Seeds as Possible Predictors of
426 Extractable Phenolic Compounds. *J. Agric. Food Chem.*, *61*, 8752-8764.
- 427 32. Rustioni, L. (2017). Oxidized Polymeric Phenolics: Could They Be Considered
428 Photoprotectors? *J. Agric. Food Chem.*, *65*, 7843–7846.
- 429 33. Rustioni, L., & Failla, O. (2016). Grape seed ripening evaluation by ortho-diphenol
430 quantification. *Ital. J. Food Sci.*, *28*, 510-516.
- 431 34. Rustioni, L., Basilico, R., Fiori, S., Leoni, A., Maghradze, D., & Failla, O. (2013a). Grape
432 colour phenotyping: development of a method based on the reflectance spectrum. *Phytochem.*
433 *Anal.*, *24*, 453–459.
- 434 35. Rustioni, L., Ciacciulli, A., Grossi, D., Brancadoro, L., & Failla, O. (2016). Stem Xylem
435 Characterization for *Vitis* Drought Tolerance. *J Agric Food Chem*, *64*, 5317–5323.
- 436 36. Rustioni, L., Di Meo, F., Guillaume, M., Failla, O., & Trouillas, P. (2013b). Tuning color
437 variation in grape anthocyanins at the molecular scale. *Food Chem.*, *141*, 4349–4357.
- 438 37. Rustioni, L., Rocchi, L., Guffanti, E., Cola, G., & Failla, O. (2014). Characterization of grape
439 (*Vitis vinifera* L.) berry sunburn symptoms by reflectance. *J. Agric. Food Chem.*, *62*, 3043–
440 3046.

- 441 38. Schultze, S.R., Sabbatini, P., & Luo, L. (2016). Effects of a warming trend on cool climate
442 viticulture in Michigan, USA. *SpringerPlus* 5 (1), 1-15.
- 443 39. Waterhouse, A.L., & Laurie, V.F. (2006). Oxidation of wine phenolics: a critical evaluation
444 and hypotheses. *Am. J. Enol. Vitic.*, 57(3), 306-313.
- 445 40. Zanchi, D., Vernhet, A., Poncet-Legrand, C., Cartalade, D., Tribet, C., Schweins, R., & Cabane,
446 B. (2007). Colloidal Dispersions of Tannins in Water-Ethanol Solutions. *Langmuir*, 23, 9949-
447 9959.

448 TABLES

449

450 Table 1: Michigan seed color variations (Lightness: L*; Chroma: C*; hue: h*) in different sampling times during natural ripening (1a) and as a consequence of
 451 freeze-thaw treatment with respect to the pre-treatment values – control (1b) in terms of average values and of each cultivar.

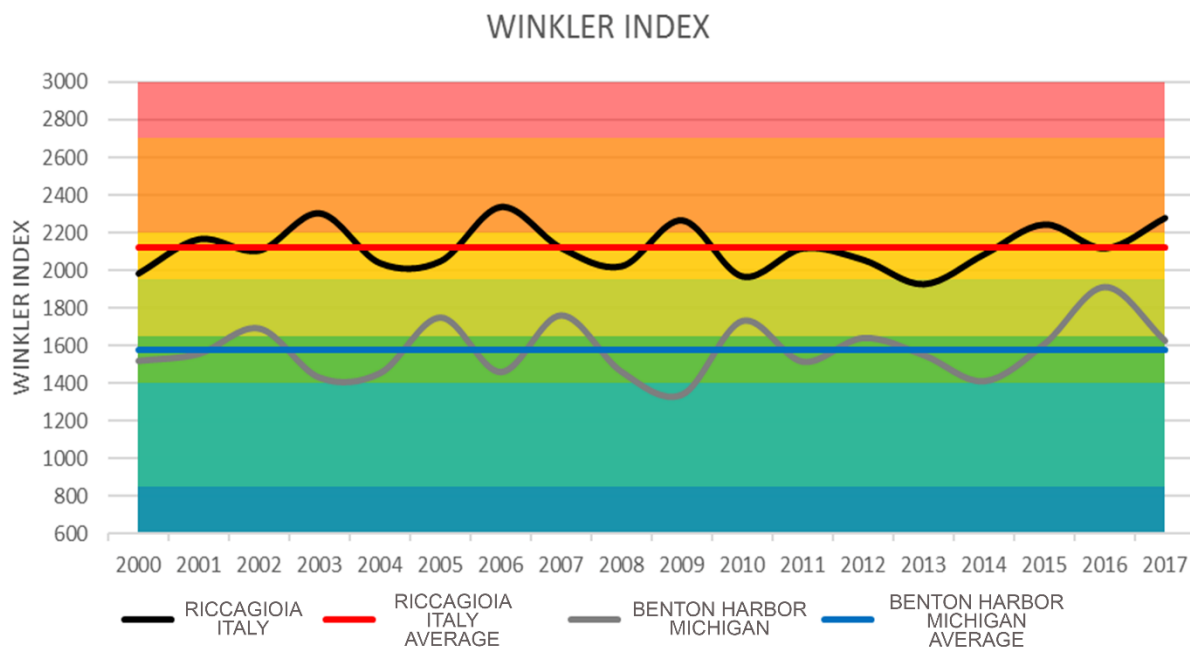
Table 1a		L*	Trend	Sig.	C*	Trend	Sig.	h*	Trend	Sig.	
Average of all the cultivars	1st sample	73.66 ± 4.35	↗	0.000	6.08 ± 2.29	↗	0.000	71.53 ± 12.33	↗	0.000	
	2nd sample	77.54 ± 5.21			7.66 ± 1.58			79.21 ± 5.03			
Cabernet Franc	1st sample	75.73 ± 4.09	=	0.139	7.14 ± 2.11	↗	0.093	71.32 ± 5.86	↗	0	
	2nd sample	77.09 ± 5.00			7.75 ± 1.41			76.66 ± 4.99			
Cabernet Sauvignon	1st sample	74.44 ± 3.68	↗	0	6.64 ± 1.85	↗	0.017	85.25 ± 8.31	↘	0.005	
	2nd sample	79.06 ± 4.94			7.42 ± 1.30			81.44 ± 4.54			
Chambourcin	1st sample	71.02 ± 5.55	↗	0.007	3.33 ± 1.05	↗	0.000	54.35 ± 7.89	↗	0.000	
	2nd sample	74.12 ± 5.70			6.22 ± 1.30			80.18 ± 5.29			
Merlot	1st sample	74.81 ± 2.75	↗	0.000	6.13 ± 1.47	↗	0.000	73.61 ± 7.27	↗	0.000	
	2nd sample	78.95 ± 3.74			8.43 ± 1.11			80.32 ± 4.43			
Pinot noir	1st sample	72.31 ± 3.49	↗	0	7.17 ± 2.26	↗	0.001	73.10 ± 7.33	↗	0	
	2nd sample	78.47 ± 4.97			8.47 ± 1.61			77.43 ± 4.29			
Table 1b		L*	Trend	Sig.	C*	Trend	Sig.	h*	Trend	Sig.	
Average of all the cultivars	1st sample	control	73.66 ± 4.35	↘	0.013	6.08 ± 2.29	↘	0.000	71.53 ± 12.33	↘	0.000
		treated	72.67 ± 4.56			5.26 ± 1.74			60.97 ± 8.10		

	2nd sample	control	77.54 ± 5.21	⋮	0.000	7.66 ± 1.58	⋮	0.000	79.21 ± 5.03	⋮	0.000
		treated	74.86 ± 4.59			6.34 ± 1.59			73.67 ± 6.13		
Cabernet Franc	1st sample	control	75.73 ± 4.09	⋮	0.030	7.14 ± 2.11	⋮	0.013	71.32 ± 5.86	⋮	0.000
		treated	73.94 ± 4.02			6.17 ± 1.68			59.44 ± 4.38		
	2nd sample	control	77.09 ± 5.00	⋮	0.000	7.75 ± 1.41	⋮	0.000	76.66 ± 4.99	⋮	0.000
		treated	73.50 ± 3.80			6.62 ± 1.43			69.98 ± 5.68		
Cabernet Sauvignon	1st sample	control	74.44 ± 3.68	⋮	0.000	6.64 ± 1.85	⋮	0.001	85.25 ± 8.31	⋮	0.000
		treated	71.14 ± 3.61			5.52 ± 1.47			70.93 ± 7.57		
	2nd sample	control	79.06 ± 4.94	⋮	0.010	7.42 ± 1.30	⋮	0.000	81.44 ± 4.54	⋮	0.000
		treated	76.51 ± 4.67			6.07 ± 1.40			77.51 ± 4.53		
Chambourcin	1st sample	control	71.02 ± 5.55	=	0.946	3.33 ± 1.05	↗	0.014	54.35 ± 7.89	↗	0.000
		treated	70.96 ± 4.60			3.83 ± 0.93			59.90 ± 7.18		
	2nd sample	control	74.12 ± 5.70	=	0.408	6.22 ± 1.29	⋮	0.000	80.18 ± 5.29	⋮	0.084
		treated	75.12 ± 6.33			4.93 ± 1.46			78.07 ± 6.76		
Merlot	1st sample	control	74.81 ± 2.75	=	0.974	6.13 ± 1.47	⋮	0.005	73.16 ± 7.27	⋮	0.000
		treated	74.78 ± 4.36			5.23 ± 1.68			59.80 ± 5.69		
	2nd sample	control	78.95 ± 3.74	⋮	0.000	8.43 ± 1.11	⋮	0.000	80.32 ± 4.43	⋮	0.000
		treated	76.11 ± 3.26			6.54 ± 1.11			73.34 ± 3.71		
Pinot noir		control	72.13 ± 3.49	=	0.801	7.17 ± 2.26	⋮	0.000	73.10 ± 7.33	⋮	0.000

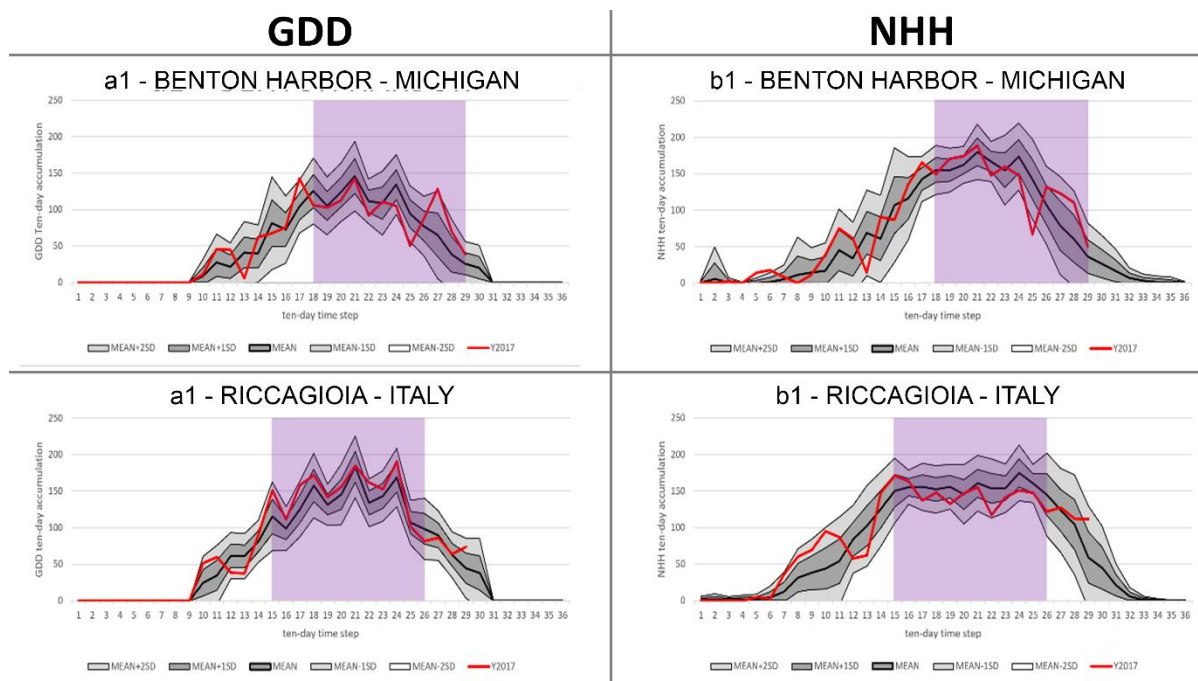
	1st sample	treated	72.53 ± 4.99			5.54 ± 1.92			54.76 ± 5.25		
	2nd sample	control	78.47 ± 4.97	↘	0.000	8.47 ± 1.61	↘	0.002	77.43 ± 4.29	↘	0.000
		treated	73.03 ± 3.22			7.55 ± 1.35			69.46 ± 3.42		

452

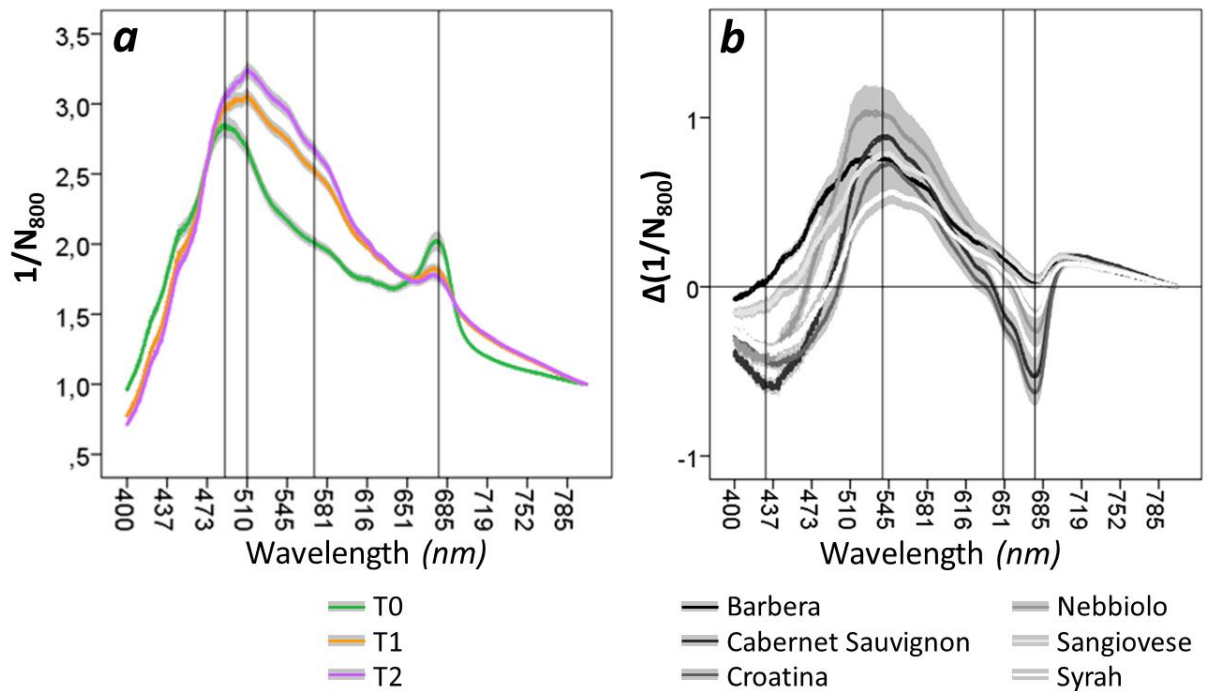
453



455
 456 Figure 1: Yearly Winkler Index from 2000 to 2017 in Riccagioia (Italy) and Benton Harbor (USA-
 457 Michigan). Average values are also presented. The chart is divided into the seven Winkler classes (I-
 458 I, II, III, IV, V and V+).



459
 460 Figure 2: GDD (Winkler Growing Degree Days) and NHH (Normal Heat Hours) behavior during
 461 2017 in Benton Harbor (USA-Michigan) and Riccagioia (Italy). Purple areas represent the timespan
 462 between fruit set and maturity.



463

464

465

466

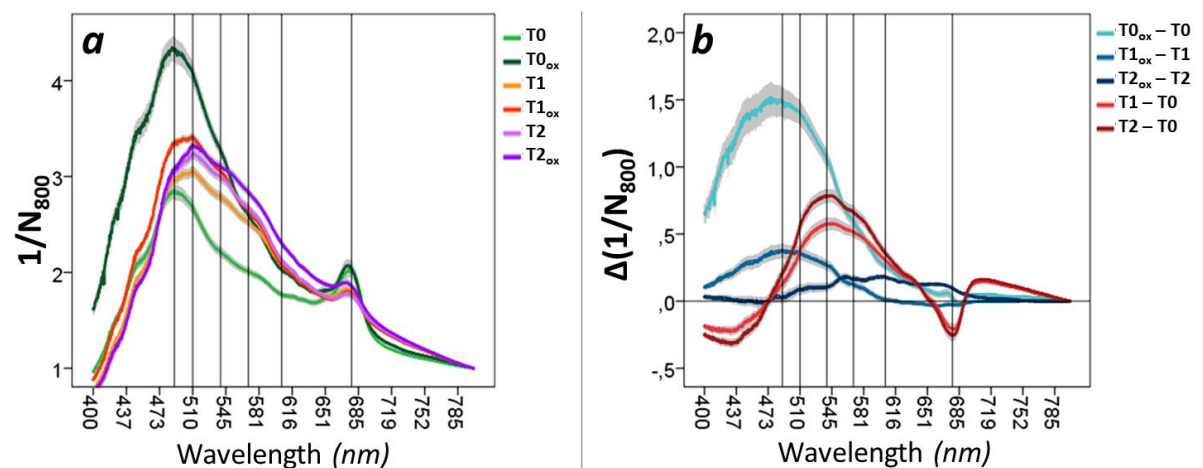
467

468

469

470

Figure 3: Variations of reflectance spectra in the Italian seed samples during natural ripening. In figure 1a, the spectra are presented as average values of all the cultivars at veraison (T0 - BBCH 83); middle ripening (T1 - BBCH 86); and harvest time (T2 - BBCH 89). Vertical bars are in correspondence of 490 nm; 510 nm; 570 nm and 678 nm. In figure 1b, the differential spectra ($\Delta(1/N_{800})$) between T2 and T0 samples of each cultivar are shown. Positive values indicate pigment accumulation, while negative values reveal pigment loss. Vertical bars are in correspondence of 430 nm; 540 nm; 650 nm and 678 nm. The line thickness is representative of the error bars (95% CI).



471

472

473

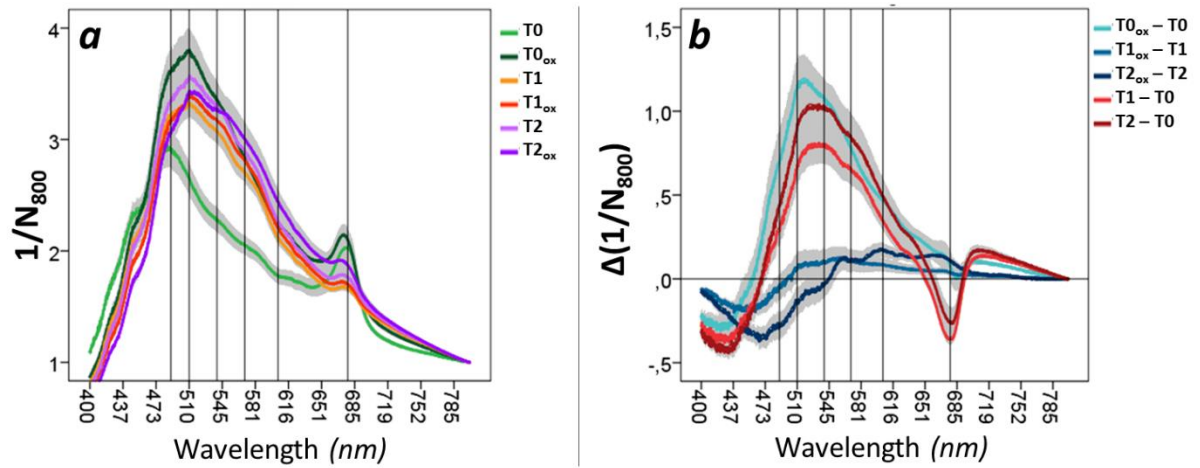
474

475

476

477

Figure 4: Variations of reflectance spectra in the Italian seed samples as a result of a freeze-thaw treatment. Data are reported as average values of all the cultivars. Figure 2a shows the average seed spectra before and after treatment in the three sampling times. In figure 2b, the spectral variations are presented as differential spectra ($\Delta(1/N_{800})$), to facilitate the comparison among natural and artificial ripening effects. Vertical bars are in correspondence of 490 nm; 510 nm; 540 nm; 570 nm; 605 nm; 678 nm. The line thickness is representative of the error bars (95% CI).



478

479

480

481

482

483

484

485

Figure 5: Variations of reflectance spectra in Nebbiolo seed samples as a result of a freeze-thaw treatment. Figure 2a shows the average seed spectra before and after treatment in the three sampling times. In figure 2b, the spectral variations are presented as differential spectra ($\Delta(1/N_{800})$), to facilitate the comparison among natural and artificial ripening effects. Vertical bars are in correspondence of 490 nm; 510 nm; 540 nm; 570 nm; 605 nm; 678 nm. The line thickness is representative of the error bars (95% CI).